

Supplementary Information

Mixed-valent nonanuclear [Mn^{II}₅Mn^{III}₄] molecular cluster with cubic topology of highest symmetry as bifunctional electrocatalyst for efficient water splitting

Chandan Sarkar,^a Tapan Sarkar,^a Aditi De,^b Nityananda Dutta,^a Julia Klak,^c Allen G. Oliver,^d Ranjay K. Tiwari,^e J. N. Behera,^e Subrata Kundu*,^b and Manindranath Bera*^a

^aDepartment of Chemistry, University of Kalyani, Nadia, West Bengal-741235, INDIA.

^bProcess Engineering (EPE) Division, Central Electrochemical Research Institute, Karaikudi-630006, Tamil Nadu, INDIA, and Academy of Scientific and Innovative Research (AcSIR), Ghaziabad-201002, INDIA.

^cFaculty of Chemistry, University of Wroclaw, Wroclaw 50383, POLAND.

^dDepartment of Chemistry and Biochemistry, University of Notre Dame, Notre Dame, IN 46556-5670, USA.

^eSchool of Chemical Sciences, National Institute of Science Education & Research, An OCC of Homi Bhabha National Institute, Bhubaneswar, Khurda, Odisha-752050, INDIA.

Determination of turnover frequency (TOF) of catalyst 1 for OER from the redox features of CV:

Calculated area acquired from C_{dl} curve considering low scan rate of 30 mV/sec = 0.00913 mVAcm⁻²

$$\begin{aligned}\text{Hence, the associated charge} &= 0.00913 \text{ mVAcm}^{-2} / 30 \text{ mVs}^{-1} \\ &= 0.0003043 \text{ Asc m}^{-2} \\ &= \mathbf{0.0003043 \text{ Ccm}^{-2}}\end{aligned}$$

$$\begin{aligned}\text{Now, the number of electrons transferred} &= 0.0003043 \text{ Ccm}^{-2} / 1.602 \times 10^{-19} \text{ C} \\ &= \mathbf{0.190 \times 10^{15} \text{ cm}^{-2}}\end{aligned}$$

The corresponding expression to determine Turnover Frequency (TOF) from OER current density is,

$$TOF = \frac{j \times N_A}{n \times F \times \tau} \dots \dots \dots (S1)$$

where, j = current density, N_A = Avogadro number, F = Faraday constant, n = number of electrons for OER = 4, Γ = surface concentration.

Hence, we have,

$$\begin{aligned}TOF_{1.74 \text{ V}} &= [(0.126) \text{ Acm}^{-2}(6.023 \times 10^{23}) \text{ mol}^{-1}] / [(96485) \text{ Cmol}^{-1} (4) (0.190 \times 10^{15}) \text{ cm}^{-2}] \\ &= \mathbf{1034 \text{ sec}^{-1}}\end{aligned}$$

Determination of turnover frequency (TOF) of catalyst 1 for HER from the redox features of CV:

Calculated area acquired from C_{dl} curve considering low scan rate of 30 mV/sec = 0.000836 mVAcm⁻²

Hence, the associated charge = 0.000836 mVAcm⁻² / 30 mVs⁻¹

$$= 0.00002786 \text{ Asc m}^{-2}$$

$$= \mathbf{0.00002786 \text{ Ccm}^{-2}}$$

Now, the number of electrons transferred = 00002786 Ccm⁻² / 1.602 × 10⁻¹⁹ C

$$= \mathbf{0.174 \times 10^{15} \text{ cm}^{-2}}$$

The corresponding expression to determine Turnover Frequency (TOF) from HER current density is,

$$TOF = \frac{j \times N_A}{n \times F \times \tau} \dots \dots \dots (S1)$$

where, j = current density, N_A = Avogadro number, F = Faraday constant, n = number of electrons for HER =2, Γ = surface concentration.

Hence, we have,

$$\begin{aligned} TOF_{-0.423 \text{ V}} &= [(0.078) \text{ Acm}^{-2}(6.023 \times 10^{23}) \text{ mol}^{-1}] / [(96485) \text{ Cmol}^{-1} (2) (0.174 \times 10^{15}) \text{ cm}^{-2}] \\ &= \mathbf{1390 \text{ sec}^{-1}} \end{aligned}$$

Figures with captions

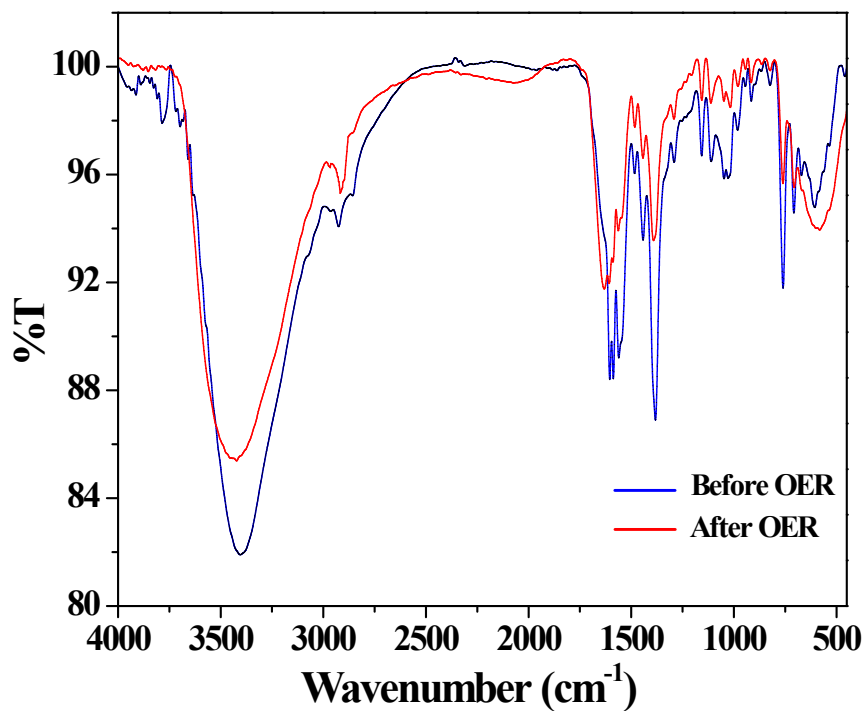


Fig. S1. FTIR spectra of **1** in the region of 4000-450 cm^{-1} before (—) and after (—) OER.

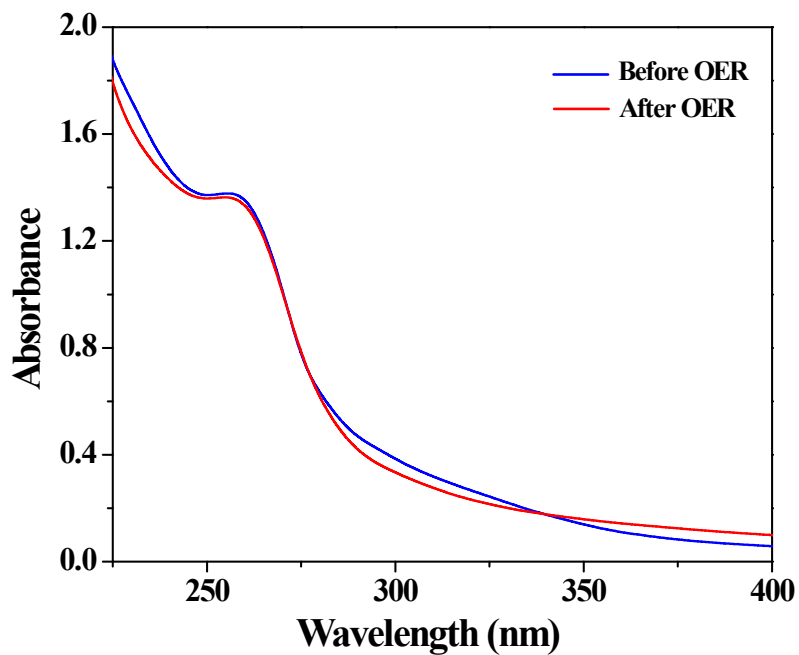


Fig. S2. UV-Vis spectra of **1** at 10^{-4} (M) in aqueous solution before (—) and after (—) OER.

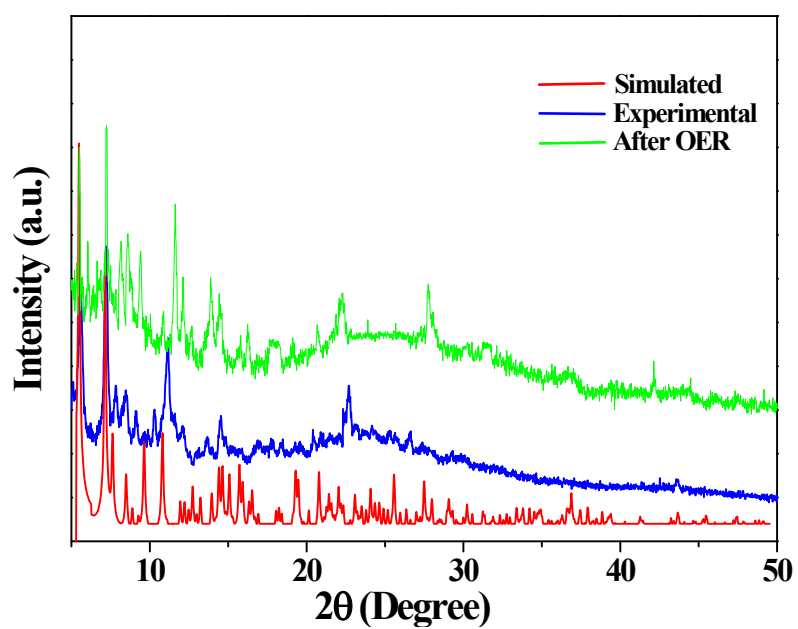
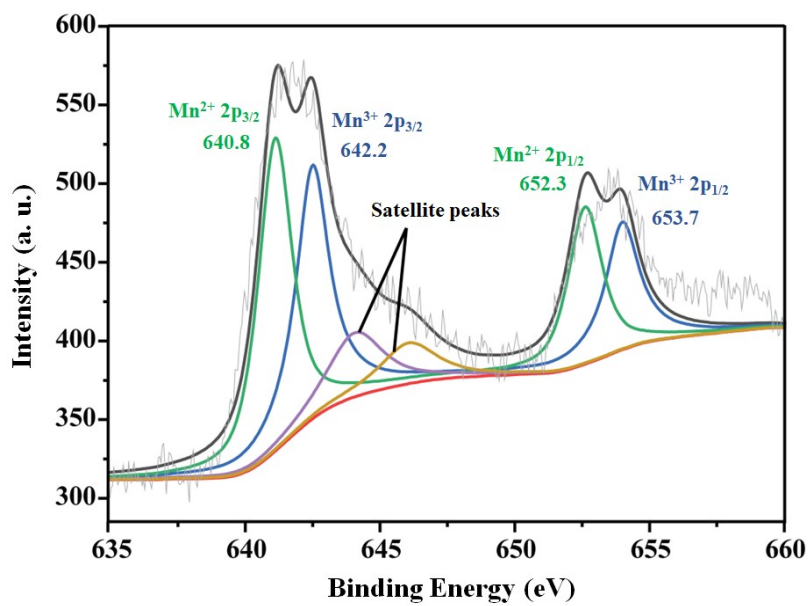
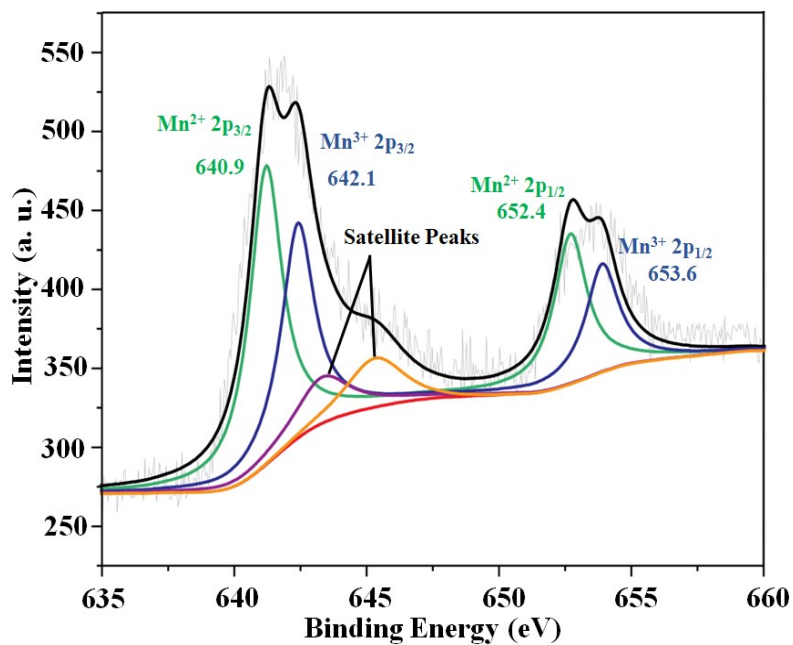


Fig. S3. Powder X-ray diffraction (PXRD) patterns of **1**: simulated PXRD (—), and experimental PXRD before (—) and after (—) OER.



(a)



(b)

Fig. S4. X-ray photoelectron spectra (XPS) of the manganese 2p level in **1** (a) before and (b) after OER.

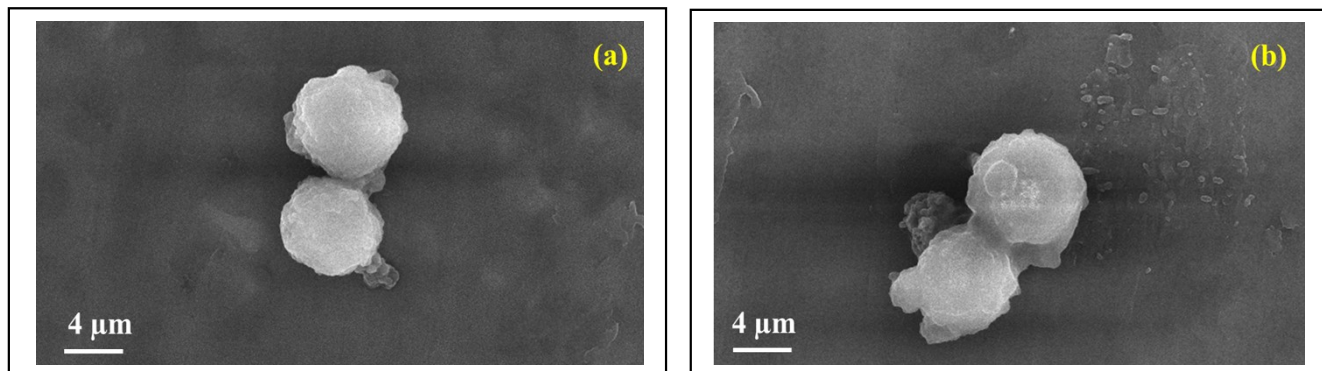


Fig. S5. Field emission scanning electron microscopic (FESEM) images of **1** (a) before and (b) after OER.

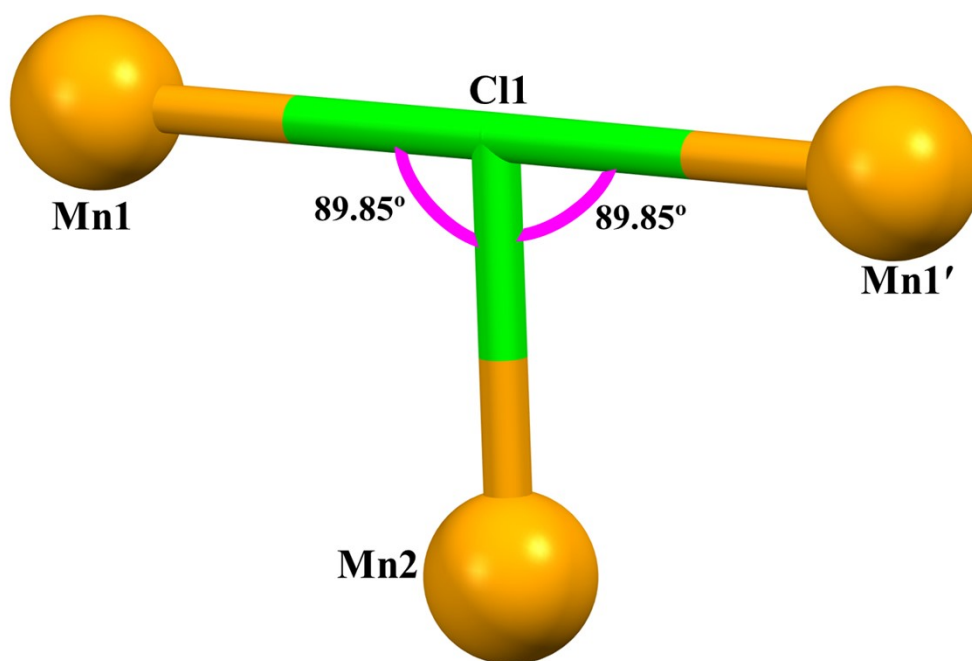


Fig. S6. Arrangement of Mn1, Mn2 and Mn1' atoms with C11 atom in **1** making a T-shaped geometry.

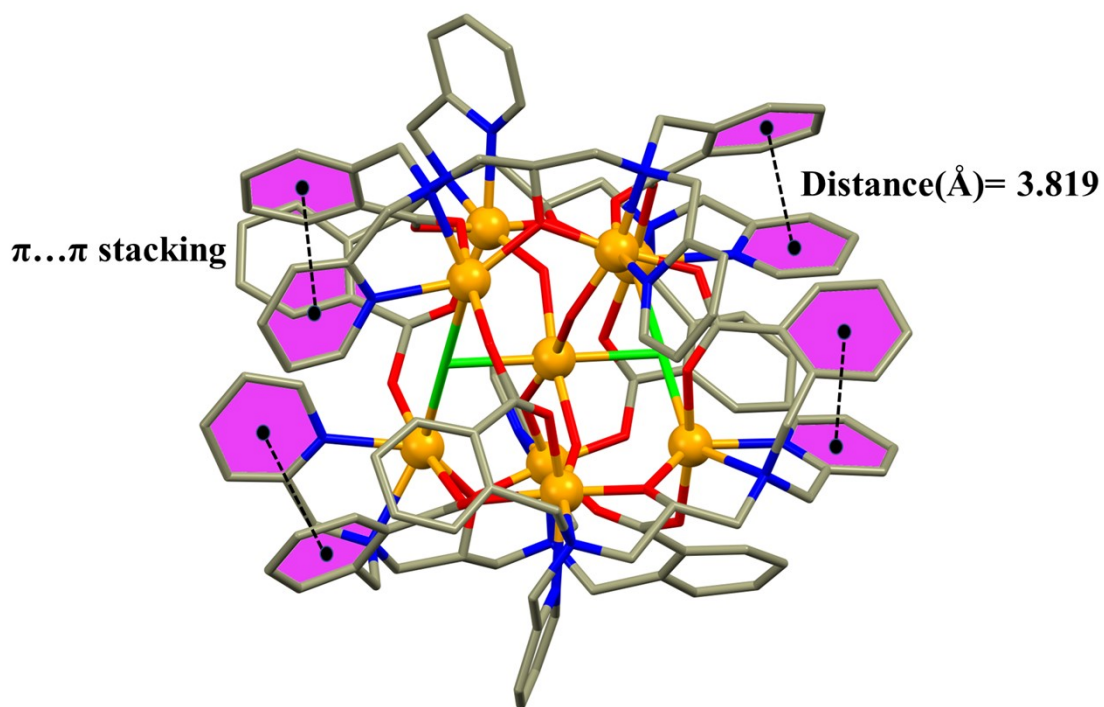


Fig. S7. A view of **1** showing intra-molecular $\pi \dots \pi$ stacking interactions.

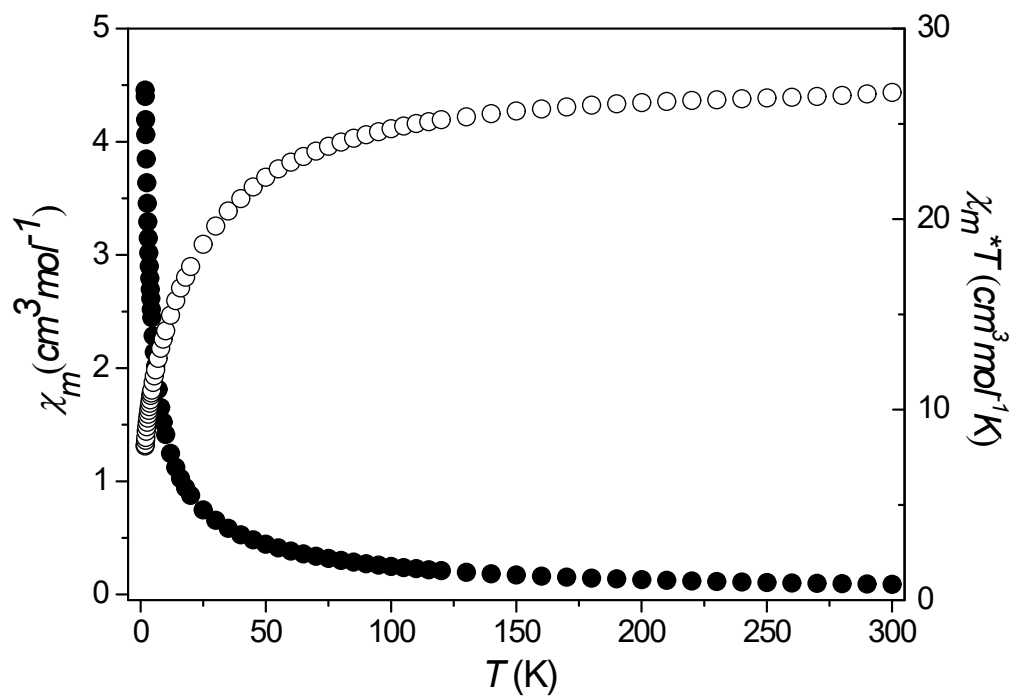


Fig. S8. Temperature dependence of χ_m (●) and $\chi_m T$ (○) (χ_m per $\text{Mn}^{\text{II}}_5\text{Mn}^{\text{III}}_4$ unit) for **1**.

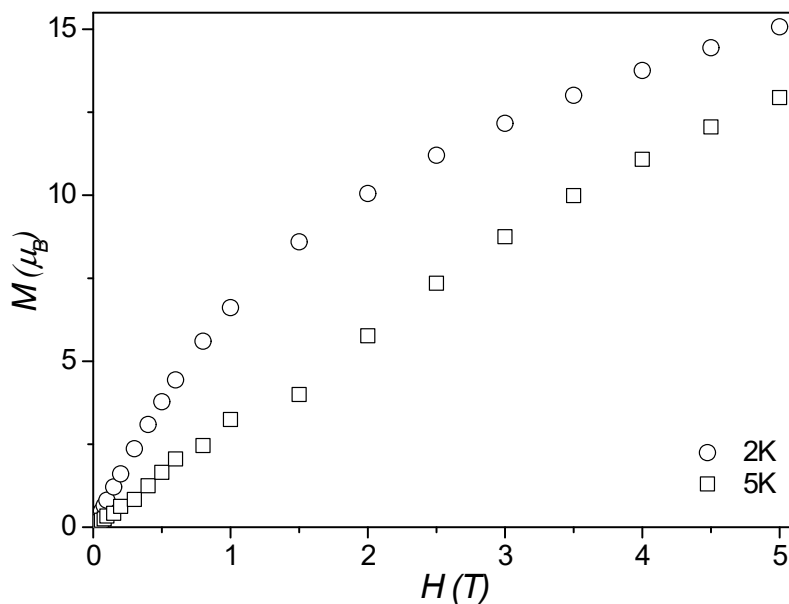


Fig. S9. Field (H) dependence of the magnetization (M) (magnetization per $\text{Mn}^{\text{II}}_5\text{Mn}^{\text{III}}_4$ unit) for **1** at 2 and 5 K.

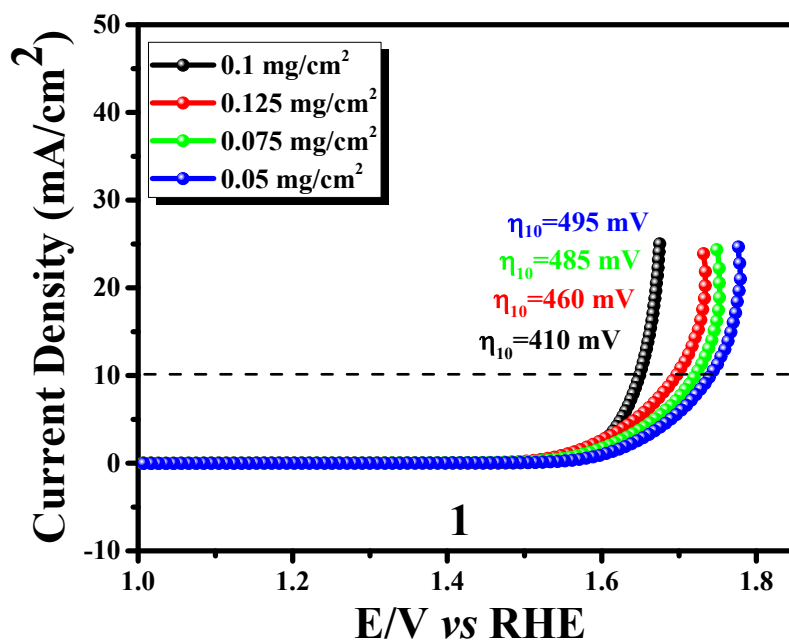


Fig. S10. Mass loading dependency of **1** for OER studies.

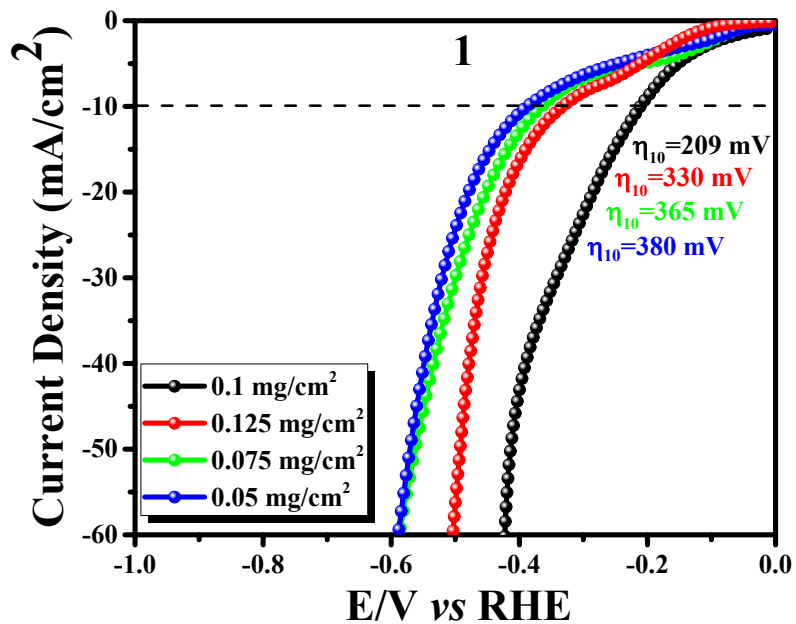


Fig. S11. Mass loading dependency of **1** for HER studies.

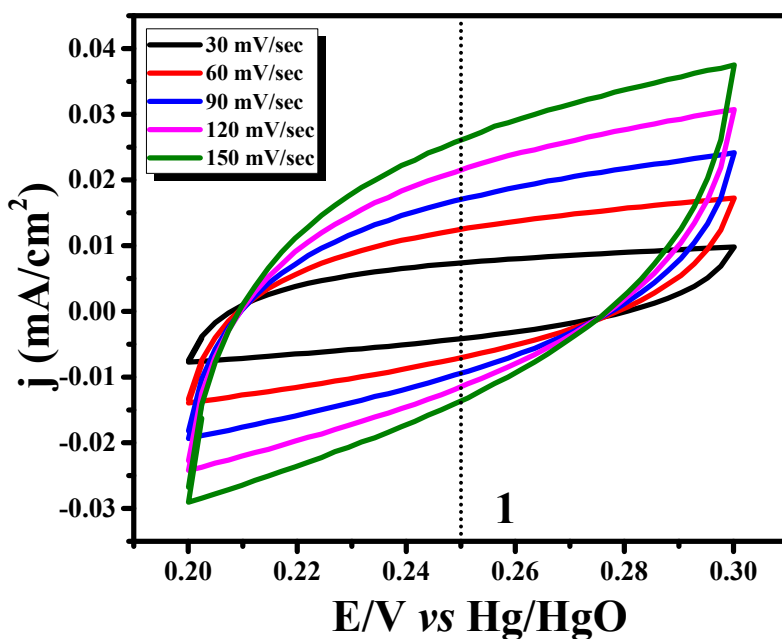


Fig. S12. CV outcomes of **1** under non-Faradaic region with various scan rates in OER studies.

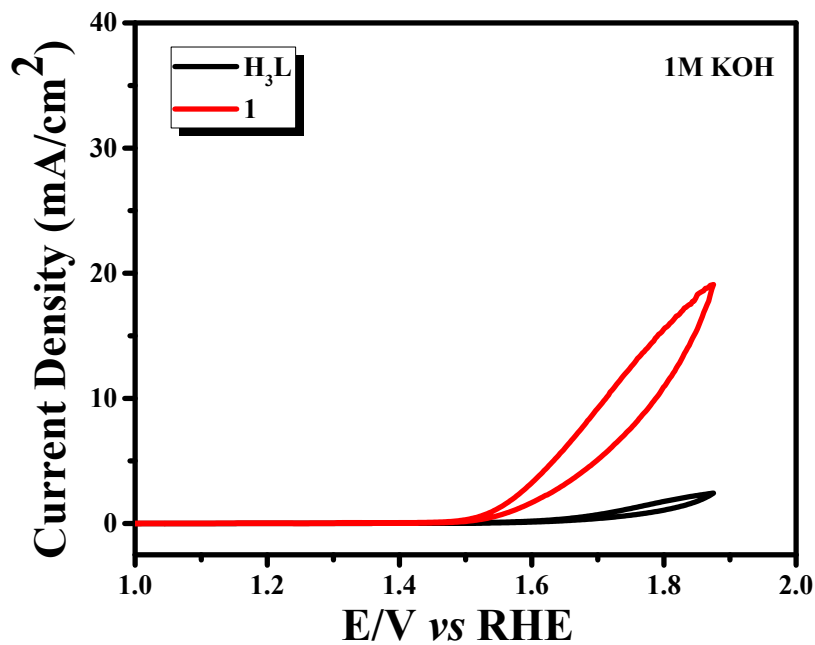


Fig. S13. CV outcomes of H₃L and cluster 1 in 1M KOH alkaline medium for OER studies.

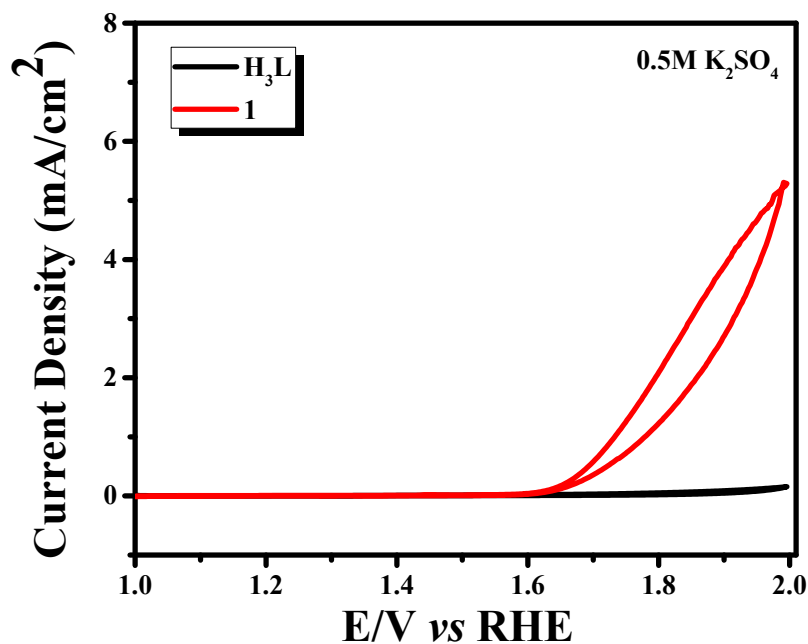


Fig. S14. CV outcomes of H₃L and cluster 1 in 0.5M K₂SO₄ neutral medium for OER studies.

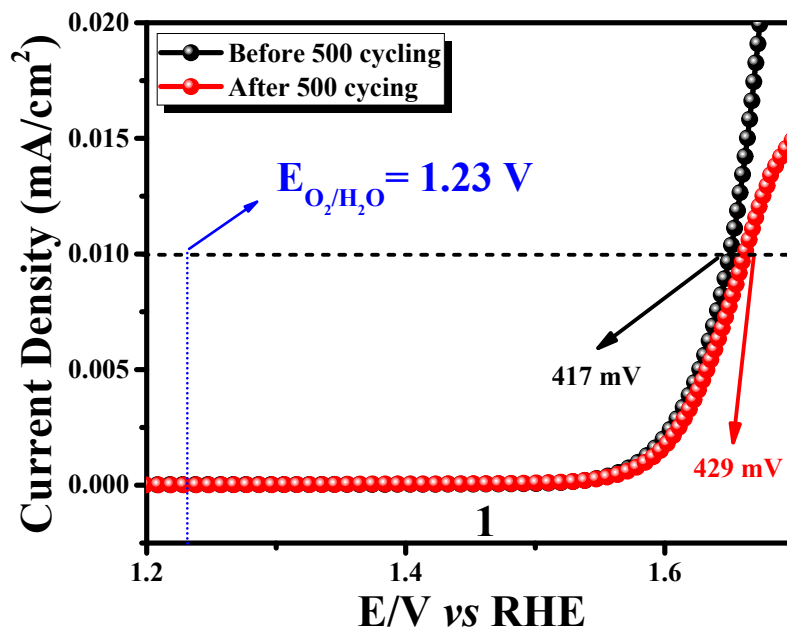


Fig. S15. LSV outcomes of 1 before and after OER AD studies.

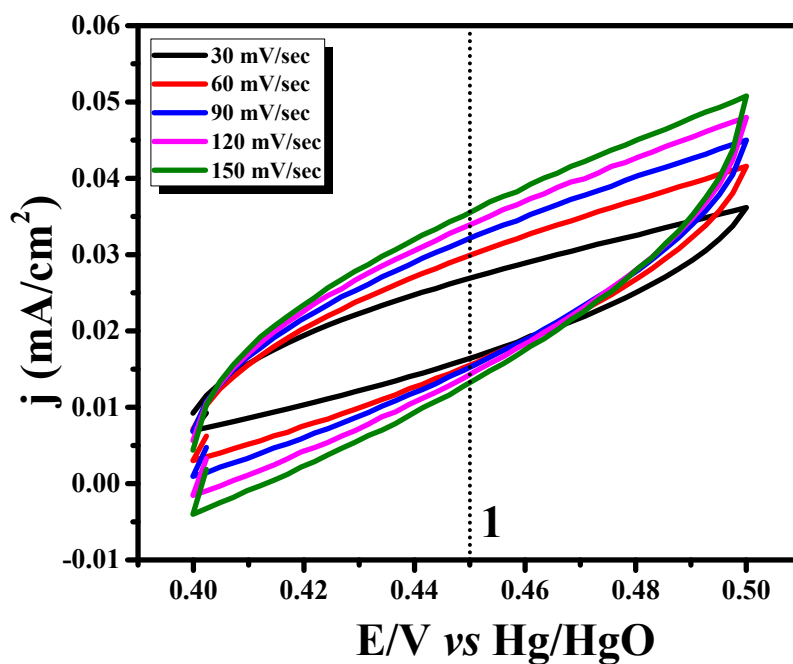


Fig. S16. CV outcomes of 1 under non-Faradaic region with various scan rates in HER studies.

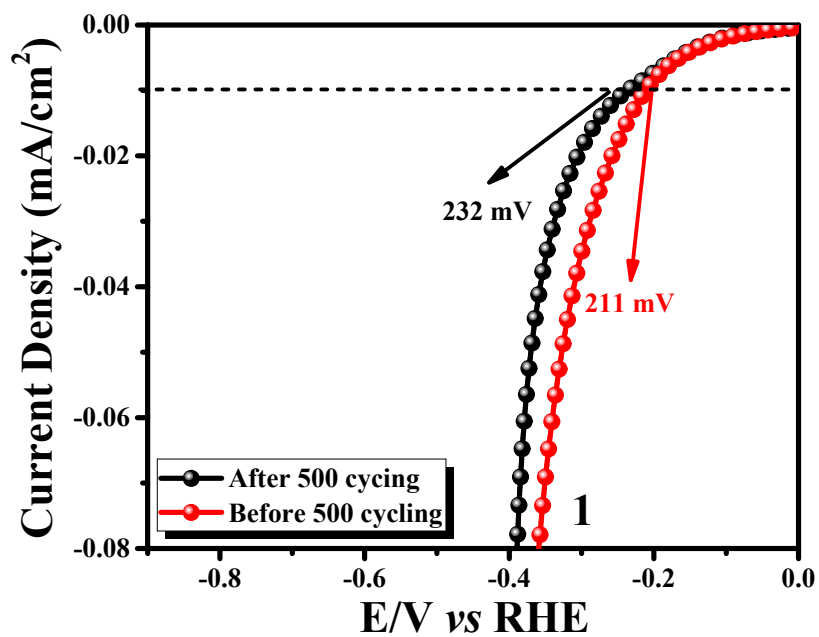


Fig. S17. LSV outcomes of 1 before and after HER AD studies.

Tables with captions

Table S1. Crystal data and refinement parameters for [Mn ₉ L ₄ (μ ₂ -O) ₄ (μ ₃ -Cl) ₂] (1)	
Empirical formula	C ₁₂₄ H ₁₁₆ N ₁₆ O ₂₄ Cl ₂ Mn ₉
Formula weight	2779.689
Crystal system	cubic
Space group	<i>Ia-3d</i>
<i>a</i> , Å	48.362(2)
<i>b</i> , Å	48.362(2)
<i>c</i> , Å	48.362(2)
<i>α</i> , deg	90
<i>β</i> , deg	90
<i>γ</i> , deg	90
Volume, Å ³	113112(9)
<i>Z</i>	24
Density (calculated), Mg/m ³	0.979
Wavelength, Å	1.54178
Temperature, K	154.00
<i>F</i> (000)	34152
Absorption coefficient, mm ⁻¹	5.414
<i>θ</i> range for data collection, deg	2.238 to 31.362
Reflections collected	1534
Independent reflections	1362
<i>R</i> (<i>F</i> obsd data) [<i>I</i> > 2σ(<i>I</i>)]	0.0945
<i>wR</i> (<i>F</i> ² all data)	0.2610
Goodness-of-fit on <i>F</i> ²	1.102
Largest diff. peak and hole, e/Å ³	+0.376 to -0.443

$$wR2 = \{\sum [w(F_o^2 - F_c^2)^2] / \sum [w(F_o^2)^2]\}^{1/2} R1 = \sum ||F_o| - |F_c|| / \sum |F_o|$$

Table S2. Selected bond distances (Å) and angles (deg) for [Mn₉(L)₄(μ₂-O)₄(μ₃-Cl)₂] (**1**)

Bond distances (Å)			
Mn(1)-O(1)	2.103(16)	Mn(2)-Cl(1)	2.537(10)
Mn(1)-O(2)	2.178(18)	Mn(3)-O(1)	1.890(17)
Mn(1)-O(5)	2.19(2)	Mn(3)-O(3)	1.89(2)
Mn(1)-N(1)	2.44(2)	Mn(3)-O(4)	2.176(17)
Mn(1)-N(2)	2.33(2)	Mn(3)-O(6)	1.921(15)
Mn(1)-Cl(1)	2.777(4)	Mn(3)-N(3)	2.13(2)
Mn(2)-O(6)	2.192(13)	Mn(3)-N(4)	2.29(2)
Bond angles (deg)			
O(1)-Mn(1)-O(2)	84.2(6)	O(6)-Mn(2)-O(6')	90.29(5)
O(1)-Mn(1)-O(5)	92.5(6)	Cl(1)-Mn(2)-Cl(1')	180.0
O(1)-Mn(1)-N(1)	71.5(7)	O(1)-Mn(3)-O(3)	173.1(8)
O(1)-Mn(1)-N(2)	138.3(8)	O(1)-Mn(3)-O(4)	94.9(6)
O(1)-Mn(1)-Cl(1)	135.3(5)	O(1)-Mn(3)-O(6)	82.4(7)
O(2)-Mn(1)-O(5)	173.3(7)	O(1)-Mn(3)-N(3)	82.0(8)
O(2)-Mn(1)-N(1)	79.2(7)	O(1)-Mn(3)-N(4)	96.3(7)
O(2)-Mn(1)-N(2)	105.5(7)	O(3)-Mn(3)-O(4)	84.9(7)
O(2)-Mn(1)-Cl(1)	79.1(5)	O(3)-Mn(3)-O(6)	104.5(7)
O(5)-Mn(1)-N(1)	105.3(8)	O(3)-Mn(3)-N(3)	91.1(8)
O(5)-Mn(1)-N(2)	80.9(7)	O(3)-Mn(3)-N(4)	81.9(7)
O(5)-Mn(1)-Cl(1)	99.5(6)	O(4)-Mn(3)-O(6)	93.8(6)
N(1)-Mn(1)-N(2)	70.8(9)	O(4)-Mn(3)-N(3)	87.6(8)
N(1)-Mn(1)-Cl(1)	142.6(6)	O(4)-Mn(3)-N(4)	159.0(7)
N(2)-Mn(1)-Cl(1)	86.3(7)	O(6)-Mn(3)-N(3)	164.3(8)
O(6)-Mn(2)-Cl(1)	94.1(4)	O(6)-Mn(3)-N(4)	105.3(7)
O(6')-Mn(2)-Cl(1)	85.9(4)	N(3)-Mn(3)-N(4)	76.4(8)

Table S3. Overpotential (η) and current density (j) values of some reported metal oxide- or metal chelate-based electrocatalysts towards oxygen evolution reaction (OER)

Sl. No.	Metal Oxide/Metal Chelate-Based Electrocatalysts	Overpotential (η) (mV)	Current Density (j) (mA/cm ²)	Ref.
1.	MnO ₂ -Ni _{0.002(M)}	445	10	53
2.	Carbon Dots 0.15-MnO ₂	343	10	54
3.	urchin-like α -MnO ₂	640	-	55
4.	Co-intercalated layered MnO ₂	360	10	56
5.	α -MnO ₂ -SF	490	10	57
6.	(NMe ₄)[Cu ^{III} (L ₁)]	560	-	58
7.	[Fe ^{III} (dpaq)(H ₂ O)](ClO ₄) ₂	200-250	-	59
8.	[Mn₉L₄(μ₂-O)₄(μ₃-Cl)₂]	410	10	This Work

Table S4 Overpotential (η) and current density (j) values of some reported metal oxide- or metal chelate-based electrocatalysts towards hydrogen evolution reaction (HER)

Sl. No.	Metal Oxide/Metal Chelate-Based Electrocatalysts	Overpotential (η) (mV)	Current Density (j) (mA/cm ²)	Ref.
1.	Ni@NiL1-Sal	384	10	66
2.	[Mo ₃ S ₁₃] ²⁻ Cluster	220	10	67
3.	[Ag ₄ (S ₂ PFc(OMe) ₄) ₄]	932	5	68
4.	[MnBr(pybz)(CO) ₃]	280	10	69
5.	[{Cu ^{II} (2,2'-bpy)(H ₂ O) ₂ }] [{Co ^{II} W ^{VI} ₁₂ O ₄₀ } {Cu ^{II} (2,2'-bpy)(H ₂ O)} {Cu ^{II} (2,2'-bpy)}]·2H ₂ O	520	1	70
6.	[(UO ₂) ₂ (μ -L) ₂]	274	-	71
7.	K ₁₀ [{K ₄ (H ₂ O) ₆ } {UO ₂ } ₂ (α -PW ₉ O ₃₄) ₂]·13H ₂ O	115	1	72
8.	MnO _x /Ti	240	100	73
9.	[Mn ₉ L ₄ (μ ₂ -O) ₄ (μ ₃ -Cl) ₂]	209	10	This Work